

# X-BAND MICROWAVE UNDULATORS FOR SHORT WAVELENGTH FREE-ELECTRON LASERS \*

C. Pellegrini, University of California at Los Angeles, Los Angeles, California 90095

## Abstract

Microwave undulators have two attractive features for free-electron lasers, when compared to static magnetic undulators: the beam aperture is larger than the period; the polarization state, circular or planar, and the undulator field intensity can be changed from pulse to pulse.

High power klystrons and pulse compression techniques developed at X-band can now be used to operate microwave undulators for free-electron lasers. In this paper we discuss the parameters for X-band microwave undulators, the effect of microwave energy losses in the waveguide walls and its compensation by waveguide tapering, and the characteristics of free-electron lasers based on these systems.

## INTRODUCTION

High power microwave fields propagating in a waveguide can be used as undulators for free-electron lasers (FELs). This type of undulator -which we call TWU- has a short electron oscillation period and a large aperture for the beam propagation. Using the high power X-band sources, developed for the electron-positron linear collider, we can now build TWUs for short wavelength FELs, with a beam of lower energy and higher peak current compared to more conventional undulators.

Microwave undulators have been considered in a standing and single wave configuration [1], [2], [3], [4]. Measurements of the spontaneous undulator radiation from a 143 or 220 MeV beam in an S-band undulator have been reported [1]. A discussion of the parameters of radio frequency undulator in various configurations has been made recently in [5]. Microwave wigglers operating at 30 GHz, as damping devices in damping rings for linear colliders, has been considered in [6].

In this paper we discuss microwave undulators operating at 12 GHz. High power RF sources and pulse compression techniques, delivering about 450MW for a few hundreds of nanoseconds, have been developed near this frequency [7]. At this power level the undulator parameter is about 0.4, for a helical period of 1.45 cm and a transverse waveguide size of 1.8 cm. A conventional undulator would have a gap of about 6 mm for the same values of the period and undulator parameter. Even larger power levels can be reached using ring recirculators.

Some advantages of a TWU are: short undulator period; helical or planar electron trajectory; polarization control for each electron and radiation pulse; low level of background synchrotron radiation. However some problems must be addressed before a TWU FEL is built: reproducibility of the radio frequency power from pulse to pulse; variation in the wave amplitude and phase during the pulse; control of the change in electromagnetic

field due to wall losses; tolerances in the geometry of the waveguide. Some of these effects are discussed here.

In the following sections we evaluate the field and the electron trajectory for a TWU consisting of a rectangular waveguide, with two modes,  $m=0, n=1$  and  $m=1, n=0$ , shifted in the time phase by  $\pi/2$ . We then show that a water window FEL, 2 to 4 nm wavelength, can be built using 1 GeV linac and a TWU. At a beam energy of about 4 GeV the FEL would reach 0.15 nm. The effect of power losses in the metallic waveguide walls is discussed in the last section, showing that a small tapering of the waveguide transverse size avoids gain reduction.

## FIELDS IN THE WAVEGUIDE

Consider a waveguide with a rectangular cross section of sides  $a, b$ . The field in the waveguide is a superposition of modes characterized by two numbers,  $m$  and  $n$  [8]. We consider two transverse electric modes,  $m=0, n=1$  and  $m=1, n=0$ , with frequency  $\omega_{rf}$ , shifted in the time phase by  $\pi/2$ , and assume  $a=b$ . The reference frame has the  $z$ -axis along the waveguide axis and transverse coordinates  $\xi, \zeta$ . The fields are given by:

$$E_{x,0,1} = -i\omega_{rf}a\mu H_0 \cos(\pi\zeta/a) / \pi \times \exp[i(k_{0,1}z - \omega_{rf}t)] \quad (1)$$

$$E_{y,0,1} = 0, \quad B_{x,0,1} = 0, \quad B_{y,0,1} = \frac{k_{0,1}}{\omega_{rf}} E_{x,0,1} \quad (2)$$

$$H_{z,0,1} = -H_0 \sin(\pi\zeta/a) \exp[i(k_{0,1}z - \omega_{rf}t)] \quad (3)$$

$$E_{x,1,0} = 0, \quad B_{y,1,0} = 0, \quad B_{x,1,0} = -\frac{k_{0,1}}{\omega_{rf}} E_{y,1,0} \quad (4)$$

$$E_{y,1,0} = i\omega_{rf}a\mu H_0 \cos(\pi\xi/a) / \pi \times \exp[i(k_{0,1}z - \omega_{rf}t) + \pi/2] \quad (5)$$

$$H_{z,1,0} = -H_0 \sin(\pi\xi/a) \exp[i(k_{0,1}z - \omega_{rf}t) + \pi/2] \quad (6)$$

where

$$k_{0,1} = k_{1,0} = \pm \sqrt{(\omega_{rf}/c)^2 - (\pi/a)^2} \quad (7)$$

The cutoff frequency is  $\Omega_{1,0} = \Omega_{0,1} = \pi c/a$ . The plus or minus sign in (7) describes waves co-propagating or counter-propagating respect to the electrons. We consider only the counter-propagating case.

The power flow in the waveguide, for one mode, is

$$P = Z_0 (aH_0\omega_{rf}/\Omega_{1,0})^2 \sqrt{1 - (\Omega_{1,0}/\omega_{rf})^2} / 8 \quad (8)$$

where  $Z_0 = 120\pi\Omega$  is the vacuum impedance.

The group velocity of the field in the waveguide is

\*Work supported by DOE grant 4-444025-PG-57341.

$$V_G = c\sqrt{1 - (\Omega_{1,0} / \omega_{rf})^2}. \quad (9)$$

The power in the waveguide decreases exponentially because of energy losses in the metallic walls. The exponential attenuation length is

$$\beta_{att} = (2 + 4(\pi c / \omega_{rf} a)^2) / (a Z_0 \sigma \delta) \times \sqrt{(a \omega_{rf} / \pi c) / (1 - (\pi c / \omega_{rf} a)^2)}, \quad (10)$$

where  $\sigma$  and  $\delta$  are the metal conductivity and skin depth evaluated at the cutoff frequency,  $\delta = \sqrt{2a / \pi Z_0 \sigma}$ .

## FORCES AND TRAJECTORIES

The force due to the wave on an electron has two terms. One,  $F_w$ , due to the transverse electric and magnetic fields, produces the main wiggling motion in the undulator. The second is a defocusing force arising from the longitudinal magnetic field and the wiggling velocity. The defocusing force is nonlinear, being proportional to the particle velocity and its displacement from axis. We consider only the force producing the wiggling motion, assuming that an additional quadrupole focusing system is used to compensate the defocusing force, and focus the beam.

$$F_{w,x} / e\mu H_0 = -(a\Delta / \pi) \sin(\omega_{rf}t - k_{0,1}z) \quad (11)$$

$$F_{w,y} / e\mu H_0 = -(a\Delta / \pi) \cos(\omega_{rf}t - k_{0,1}z) \quad (12)$$

where

$$\Delta = \omega_{rf} - c\beta_z k_{0,1}. \quad (13)$$

The force decreases as one moves off the TWU axis, the opposite situation to that of a static magnetic undulator, where the field is minimum on axis.

Using (11), (12), and assuming that the electron energy is constant, the equations for the transverse motion are

$$\overset{g}{\beta}_x = -(K_0 / \gamma)\Delta \sin(\omega_{rf}t - k_{0,1}z) \quad (14)$$

$$\overset{g}{\beta}_y = -(K_0 / \gamma)\Delta \cos(\omega_{rf}t - k_{0,1}z) \quad (15)$$

where

$$K_0 = e\mu H_0 a c / \pi m c^2. \quad (16)$$

The equation for the energy change is

$$d\gamma / dt = K_0 \omega_{rf} \{ \beta_x \sin(\omega_{rf}t - k_{0,1}z) + \beta_y \cos(\omega_{rf}t - k_{0,1}z) \}. \quad (17)$$

If we assume that the energy is constant and

$$z = \beta_z c t. \quad (18)$$

the solution for the transverse velocity is

$$\beta_x = (K_0 / \gamma) \cos(\Delta t), \quad (19)$$

$$\beta_y = -(K_0 / \gamma) \sin(\Delta t). \quad (20)$$

Using (13), (7), the oscillation frequency,  $\Delta$ , is

$$\Delta = \omega_{rf} \{ 1 + \beta_z \sqrt{1 - (\pi c / \omega_{rf} a)^2} \}. \quad (21)$$

From (18)-(20), we have  $\beta_x^2 + \beta_y^2 = K_0^2 / \gamma^2$ , and from (17)  $\gamma = \text{constant}$  and

$$\beta_z = \sqrt{1 - (1 + K_0^2) / \gamma^2} = \text{constant}, \quad (22)$$

in accord with equation (18). The trajectory, given by

$$\xi = (K_0 c / \gamma \Delta) \sin(\Delta t), \quad (23)$$

$$\zeta = (K_0 c / \gamma \Delta) \cos(\Delta t), \quad (24)$$

is a helix with period

$$\lambda_U = \lambda_{rf} \beta_z / (1 + \beta_z \sqrt{1 - (\pi c / \omega_{rf} a)^2}) \quad (25)$$

where  $\lambda_{rf} = 2\pi c / \omega_{rf}$ . The ratio  $\lambda_U / \lambda_{rf}$  is between 1 and 0.5, being 1 at the cutoff frequency, for  $a = \pi c / \omega_{rf}$ , and 0.5 for  $a$  very large and relativistic electrons.

## TWU CHARACTERISTICS

The dependence of the undulator period and the undulator parameter on the waveguide size is shown in Figure 1. The RF field frequency is  $f_{rf} = 12\text{GHz}$ , and the power per mode 200MW. Reducing the waveguide size toward the cutoff value  $a = \pi c / \omega_{rf}$ , the undulator parameter increases, but at the same time the period becomes larger and the attenuation length shorter. In what follows we assume  $a = 1.8\text{cm}$ . The main characteristics for the TWU are given in Table 1. We can compare the TWU characteristics given in Table 1 with those of a hybrid type static magnetic planar undulator with the same period. For the same undulator parameter value the undulator gap would be approximately 6.4 mm.

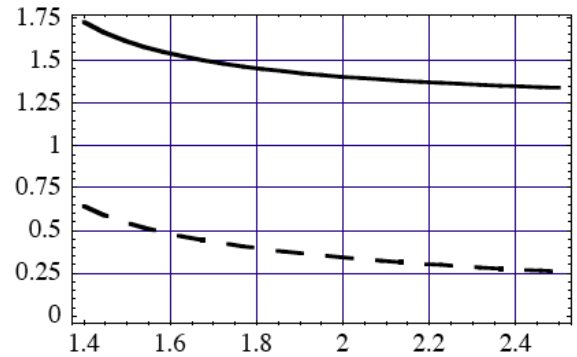


Figure 1: Undulator period, cm, solid line, and undulator parameter as a function of waveguide transverse size in cm. Input power is 200 MW per mode.

## TWU BASED FELS

For short wavelength- high gain FELs, the TWU offers the advantage of a short period and a large aperture. These features, and the reduced undulator parameter values, allow an FEL to reach shorter wavelengths for a given beam energy, with a reduced FEL saturation power. The large transverse size reduces the effect of the beam-induced wakefields, and may allow larger electron beam peak currents.

The most important FEL parameter is the gain length. Its value increases when the betatron oscillations change the phase of the electrons respect to the electromagnetic wave. However, increasing the beta function to reduce this effect reduces the electron beam density and thus increases the gain length.

Table 1: TWU characteristics.

RF frequency, GH	12
RF power, per mode , MW	200
Waveguide transverse size, a=b, cm	1.8
Equivalent undulator period, $\lambda_U$ , cm	1.45
Equivalent undulator parameter, $K_0$	.4
Attenuation coefficient, $m^{-1}$	0.028
Group velocity/c	0.72

How these two effects play is shown here for two cases. Case A is an FEL operating in the water window, from 2 to 4 nm. 2 kA peak current, 1 mm mrad normalized transverse emittance, and  $6 \times 10^5$  relative energy spread. Case B is an FEL operating near 0.1 nm, peak current 3.5kA, other parameters as in case A. The results shown in Figure 2 to Figure 4 have been calculated using the Xie FEL model [9]. The results of a Genesis [10] calculation for 3.8 GeV beam energy, and case B, are in general agreement with the Xie's model results.

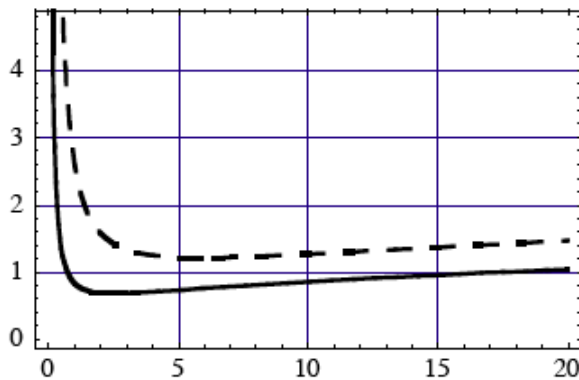


Figure 2: Gain length as a function of betatron focusing for the TWU undulator in case A. Beam energy 0.7 GeV (solid line) and 1.1 GeV.

Figure 2 shows the gain length as a function of the betatron focusing for two beam energies, corresponding to 2 and 4 nm. Figure 3 shows the gain length, saturation power and wavelength as a function of energy and for a choice of the betatron focusing  $\beta_B = 5m$ , near the minimum shown in Figure 2.

The gain length at 2 nm is about 1.5m. In case B, the shorter wavelength FEL, the results are shown in Figure 4, for an optimized betatron focusing of about 50m. A wavelength of about 0.15 nm is reached at 3.8 GeV, with a corresponding gain length of about 5 m.

In all cases considered the saturation power is smaller than for an FEL with a static planar hybrid undulator, a larger undulator parameter and beam energy.

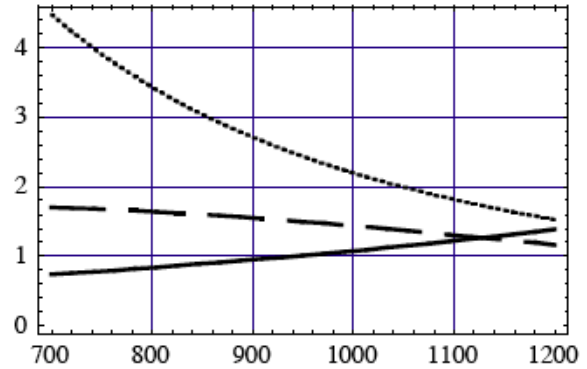


Figure 3: Gain length in m (solid line), saturation power in GW (dashed line), wavelength in nm versus energy in MeV. Case A. The betatron focusing is  $\beta_B = 5m$ .

### EFFECTS OF POWER LOSSES IN THE WAVEGUIDE WALLS

Power losses in the waveguide walls reduce the undulator parameter value and hence the radiation wavelength, changing both the spectrum and the gain. If the change is large compared with the gain width the FEL performance will be reduced. The power decreases along the waveguide as

$$P = P_0 \exp(-2\beta_{att}z), \quad (26)$$

where  $\beta_{att}$  is given by (10). The power loss decreases the radiation wavelength, and the effect can be too large for an FEL.

Power losses are estimated for a copper waveguide, with conductivity  $\sigma = 6 \times 10^7 \Omega^{-1}m^{-1}$  at room temperature. The effect is compensated changing the waveguide size along the undulator length. The wall resistivity can be reduced cooling the wall to 77 °K, liquid nitrogen temperature. Recent measurements at lower temperature at a frequency of 11.4 GHz, for a copper waveguide, show that the conductivity increases by about a factor of 3 near 77 °K, with almost no additional gain by further reducing the temperature [11]. Here we consider only the room temperature case.

The waveguide transverse size tapering is assumed as

$$a = a_0 \exp(-\alpha\beta_{att}z) \quad (27)$$

The parameter  $\alpha$  controls the amount of change.

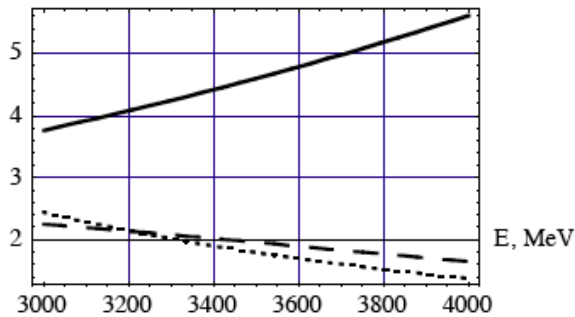


Figure 4: Gain length in m (solid line), saturation power in GW (dashed line) and wavelength in Å, for case B. Betatron focusing,  $\beta_B = 50m$ .

The effect of tapering is shown in Figure 5 and Figure 6, for  $\alpha=0, 0.17, 0.28$ , and a 10m undulator. The wavelength variation changes sign, increasing instead of decreasing, when going from  $\alpha=0.17$  to  $\alpha=0.28$ . In the last case the variation is reduced by one order of magnitude, showing that tapering is an effective way to control the wavelength change.

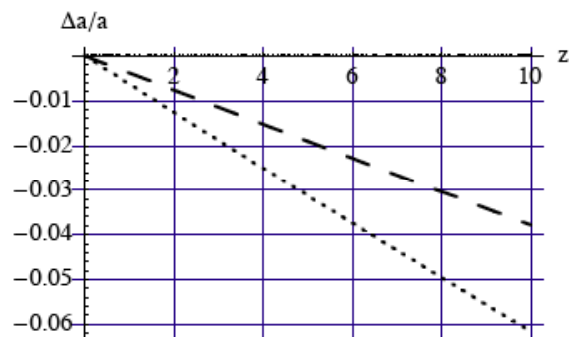


Figure 5: Relative change in the waveguide transverse size along the undulator 10 m length, for a copper waveguide at room temperature, with  $\alpha=0$  (solid line),  $\alpha=0.17$  (dashed line) and  $\alpha=0.28$ .

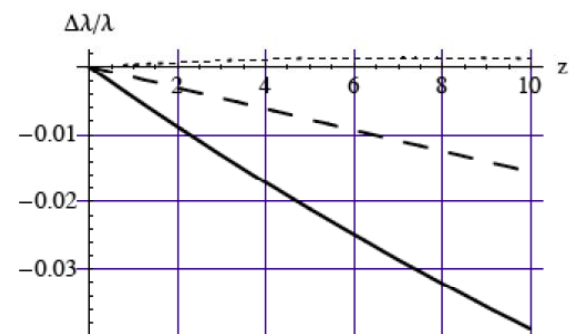


Figure 6: Relative change in wavelength. Same conditions of Figure 5.  $\alpha=0$  (solid line),  $\alpha=0.17$  (dashed line), and  $\alpha=0.28$ . Beam energy 1.05 GeV, corresponding to 2 nm.

## CONCLUSIONS

The TWU gives the advantage of short period and large aperture for short wavelength FELs. A TWU-FEL requires lower energy beam for a given wavelength, when compared to more conventional undulators. The electron trajectory can be changed from circular to planar, giving an easy way to change the polarization of the emitted wave. Changes in polarization and field amplitude, hence in wavelength, can be done from pulse to pulse.

## ACKNOWLEDGEMENTS

I wish to thank S. Reiche for the Genesis simulations, D. Robin, S. Tantawi, V. Dolgashev, C. Nantista for useful discussions. This work has been done while on sabbatical leave from UCLA to SLAC. I am grateful to John Galayda and the LCLS group for their very kind hospitality.

## REFERENCES

- [1] T. Shintake, K. Huke, J. Tanaka, I. Sato and I. Kumabe, "Development of microwave undulator", Japanese J. of Appl. Phys., 22, p. 844-851 (1983).
- [2] K. Batchelor, "Microwave Undulator", Brookhaven National Laboratory Report-12, (1983).
- [3] B. G. Danly et al., "Principles of Gyrotron Powered Electromagnetic Wigglers for Free-Electron Lasers", IEEE Journal of Quantum Electronics, Vol. QE-23, No. 1, pp. 103-116 (1987).
- [4] T.M. Tran, B.G. Danly, J. S. Wurtele, "Free-Electron Lasers with Electromagnetic Standing Wave Wigglers", IEEE J. of Quantum Electronics, Vol. QE-23, pp. 1578-1589, (1987).
- [5] M. Seidel, "Parameter Evaluation for Microwave Undulator Schemes", DESY-TESLA-FEL Report 2001-08 (2001).
- [6] H. Braun, M. Korostelev and F. Zimmerman, "Potential of Non-Standard Emittance Damping Schemes for Linear Colliders", in Proc. of the 2004 Asian Particle Accelerator Conference, TUP-11012 (2004).
- [7] S. G. Tantawi et al., "A High-power Multimode X-Band RF Pulse Compression System for Future Linear Colliders", Phys. Rev. ST Accel. Beams 8, 042002 (2005).
- [8] J. D. Jackson, Classical Electrodynamics, 3.
- [9] M. Xie, Proc. 1995 Part. Accelerator Conf., Dallas, Texas, IEEE 95CH35843, p. 183-185, (1996).
- [10] S. Reiche, "GENESIS 1.3: a fully 3D time-dependent FEL simulation code", Nuclear Instruments and Methods in Physics Research Section A, Volume 429, pp. 243-248, (1999).
- [11] S. Tantawi, private communication.